

A Concurrent Switching Model for Traffic Congestion Control

Hossein Rastgoftar, Xun Liu, and Jean-Baptiste Jeannin

Abstract—We introduce a new conservation-based approach for traffic coordination modeling and control in a network of interconnected roads (NOIR) with switching movement phase rotations at every NOIR junction. For modeling of traffic evolution, we first assume that the movement phase rotation is cyclic at every NOIR junction, but the duration of each movement phase can be arbitrarily commanded by traffic signals. Then, we propose a novel concurrent switching dynamics (CSD) with deterministic transitions among a finite number of states, representing the NOIR movement phases. We define the CSD control as a cyclic receding horizon optimization problem with periodic quadratic cost and constraints. More specifically, the cost is defined so that the traffic density is minimized and the boundary inflow is uniformly distributed over the boundary inlet roads, whereas the cost parameters are periodically changed with time. The constraints are linear and imposed by a trapezoidal fundamental diagram at every NOIR road so that traffic feasibility is assured and traffic over-saturation is avoided. The success of the proposed traffic boundary control is demonstrated by simulation of traffic congestion control in Downtown Phoenix (see Fig. 1).

Index Terms—Traffic congestion control, model predictive control, network dynamics.

I. INTRODUCTION

Traffic congestion is a prevalent global phenomenon that arose accompanied by the urbanization process, which imposes enormous costs on both economy and ecology. According to the statistical investigation, due to the traffic congestion the average annual cost for a driver in the US was 97 hours and \$1,348 in 2018 [1]. To this end, traffic management has been extensively studied by scholars in order to exploit the capacity of the existing road network such that the congestion can be alleviated without significant cost. Over the past decades, A number of approaches for traffic congestion management have been proposed, which can be roughly categorized into two groups: physics-based approaches and light-based approaches.

Physics-based approaches refer to the methods depending on the traffic model which are related with traffic flow and queue theory. Incorporating with the mass conservation law, the Cell Transmission Model (CTM) is widely applied to spatially partition a network of interconnected roads (NOIR) into road elements in the process of physics-based traffic coordination modeling [2]. Based on the CTM theory, Ba and Savla [3] propose an optimal control method to achieve

the optimal traffic flow in consideration of the traffic density of the network. Also, to analyze and control the traffic dynamics, Geroliminis and Daganzo [4] introduce the concept of macroscopic fundamental diagrams (MFD), which prove the relationship between the average traffic flow and the traffic density for urban-scale network. Since then, researchers have conducted a number of studies to integrate the MFD theory with the CTM approach, in order to enhance the accuracy of the large-scale traffic coordination model [5], [6]. Furthermore, Haddad et al. [7], [8] incorporate the perimeter control approach with the MFD theory to obtain the optimal flow of the traffic zone. Li et al. [9] introduce a feedback control strategy based on the MFD model to maximize the traffic volume of the network. In addition, model predictive control (MPC) is another prevalent approach for physics-based traffic dynamics optimization [10]–[12]. To overcome the nonlinearity of the prediction model, Lin et al. [13] rewrite the nonlinear MPC model into a mixed-integer linear programming (MILP) optimization problem and adopt the efficient MILP solver to guarantee the global optimum of the traffic flow.

Light-based approaches attempt to mitigate the traffic pressure by optimizing the timing plan of the traffic signal using model-free strategies, such as fuzzy logic, Genetic Algorithm (GA), Markov Decision Process (MDP), and neural network etc. Chiu and Chand [14] adopt the fuzzy-based strategy to control multiple intersections in a network of two-way streets with no turning motions. By collecting and processing the local traffic data, the optimization of the signal cycle length is achieved according to the degree of saturation at each intersection. Wei et al. [15] introduce a fuzzy logic approach to optimize an isolated traffic intersection with four approaches and four phases. Adjustments to the signal timing are made in response to different user’s demand for green time. Also, researchers employ the GA [16] and MDP [17], [18] approaches in the traffic signal optimization problem to reduce the traffic delay. Furthermore, with the prompt development of Artificial Intelligence (AI) technology and the breakthrough of computational capacity, Reinforcement Learning (RL) is becoming an increasingly popular data-driven approach applied for the optimization of the traffic signal plan [19]–[21]. The successful application of the RL algorithm on the optimization of the traffic signal plan presents the ability of the approach to learn through dynamic interaction with the environment. Moreover, the Deep Learning (DL) integrated RL algorithm, which is widely known as Deep Reinforcement Learning (DRL), is proposed to improve the applicability of the learning algorithm on the traffic signal optimization of the

H. Rastgoftar is with the Department of Aerospace and Mechanical Engineering at the University of Arizona, Tucson, AZ 85721, USA hrastgoftar@arizona.edu

X. Liu is with the Department of Mechanical Engineering at Villanova University, Villanova, PA 19085, USA xliu8@villanova.edu

J.-B. Jeannin is with the Department of Aerospace Engineering, University of Michigan, Ann Arbor, MI, 48109 USA jeannin@umich.edu.

large-scale NOIR [22]–[25].

This paper considers the problem of modeling and control of traffic evolution in an NOIR with movement phase rotations included at every junction. Compared with our previous work [26], the main goal is to model traffic evolution as a system with cyclic and deterministic transitions over a finite number of states representing NOIR movement phases. To this end, we assume that the movement phase rotation is periodic at every junction, but the durations of movement phases are not necessarily the same. To overcome this complexity, we propose to replace “movement phase duration” by “movement phase repetition” at every NOIR junction. To this end, we use a cycle graph with the nodes representing the movement phases, and the edges specifying transitions from the current movement phases to the next ones. Note that the cycle graph authorizes transitions to the next movement phase, which is either the same or different than the current movement phase. For traffic congestion, we assign optimal boundary inflow by solving a constrained receding horizon optimization problem with a quadratic cost function that periodically changes with time. The constraints of this boundary control problems imposing the feasibility of traffic evolution are linear and obtained by using a trapezoid fundamental diagram. Therefore, the optimal boundary inflow is obtained by solving a quadratic programming problem at every discrete time $k \in \mathbb{N}$.

This paper is organized as follows: The definitions and topology of traffic network are presented in Section II. The Problem Statement and Specification are presented in Sections III and IV, respectively, and are followed by the development of the traffic network dynamics in Section V. Traffic congestion control is presented as a periodic receding horizon optimization problem in Section VI. Simulation results are presented in Section VII, followed by Conclusion in Section VIII.

II. TRAFFIC NETWORK

We consider a NOIR with unidirectional roads defined by set \mathcal{V} and junctions defined by set \mathcal{W} . Interconnections between the roads are specified by graph $\mathcal{G}(\mathcal{V}, \mathcal{E})$ with node set \mathcal{V} and edge set $\mathcal{E} \subset \mathcal{V} \times \mathcal{V}$. Note that the set of nodes in the graph represents the set of unidirectional roads in the NOIR. In this paper, edges defined by \mathcal{E} satisfy the following two properties:

Property 1. If $(i, j) \in \mathcal{E}$, then, $(j, i) \notin \mathcal{E}$.

Property 2. If $(i, j) \in \mathcal{E}$, then, traffic is directed from $i \in \mathcal{V}$ towards $j \in \mathcal{V}$ which in turn implies that $i \in \mathcal{V}$ is the upstream road.

For every $i \in \mathcal{V}$, $\mathcal{I}_i = \{j \in \mathcal{V} : (j, i) \in \mathcal{E}\}$ and $\mathcal{O}_i = \{j \in \mathcal{V} : (i, j) \in \mathcal{E}\}$ define the in-neighbors and out-neighbors of $i \in \mathcal{V}$, respectively. In particular, the following conditions hold:

- 1) Traffic directed from $j \in \mathcal{I}_i$ towards $i \in \mathcal{V}$, if $\mathcal{I}_i \neq \emptyset$.
- 2) Traffic directed from $i \in \mathcal{V}$ towards $j \in \mathcal{O}_i$, if $\mathcal{O}_i \neq \emptyset$.

By knowing edge set \mathcal{E} , we can express \mathcal{V} as $\mathcal{V} = \mathcal{V}_{in} \cup \mathcal{V}_{out} \cup \mathcal{V}_I$ where inlet road set \mathcal{V}_{in} , outlet road set

\mathcal{V}_{out} , and interior road set \mathcal{V}_I are formally defined as follows:

$$\mathcal{V}_{in} = \{i \in \mathcal{V} : \mathcal{I}_i = \emptyset\}, \quad (1a)$$

$$\mathcal{V}_{out} = \{i \in \mathcal{V} : \mathcal{O}_i = \emptyset\}, \quad (1b)$$

$$\mathcal{V}_I = \{i \in \mathcal{V} : \mathcal{I}_i \neq \emptyset, \mathcal{O}_i \neq \emptyset\}. \quad (1c)$$

Assuming the NOIR has m junctions, $\mathcal{W} = \{1, \dots, m\}$ defines the junctions' identification numbers. At junction $i \in \mathcal{W}$, the movement phase rotation is defined by cycle graph $C_i(\mathcal{E}_i, \mathcal{R}_i)$, where $\mathcal{E}_i \subset \mathcal{E}$ and $\mathcal{R}_i \subset \mathcal{E}_i \times \mathcal{E}_i$ defines nodes and edges of cycle graph C_i . Set \mathcal{E}_i can be expressed as

$$\mathcal{E}_i = \bigcup_{j=1}^{r_i} \mathcal{E}_{i,j}, \quad \forall i \in \mathcal{W} \quad (2)$$

For better clarification of the above definitions, we consider an example NOIR of Phoenix City shown in Fig. 1 with 60 unidirectional roads identified by set $\mathcal{V} = \{1, \dots, 60\}$, where $\mathcal{V} = \mathcal{V}_{in} \cup \mathcal{V}_{out} \cup \mathcal{V}_I$, $\mathcal{V}_{in} = \{1, \dots, 11\}$, $\mathcal{V}_{out} = \{12, \dots, 22\}$, and $\mathcal{V}_I = \{23, \dots, 60\}$. The NOIR shown in Fig. 1 consists of 14 junctions defined by $\mathcal{W} = \{1, \dots, 14\}$. Set $\mathcal{E}_{12} = \mathcal{E}_{12,1} \cup \mathcal{E}_{12,2} \cup \mathcal{E}_{12,3} \cup \mathcal{E}_{12,4}$ defines the four movement phases at junction $12 \in \mathcal{W}$, where $\mathcal{E}_{12,1} = \{(2, 27), (2, 35), (2, 55)\} \subset \mathcal{E}$, $\mathcal{E}_{12,2} = \{(36, 35), (36, 27), (36, 19), (36, 55)\} \subset \mathcal{E}$, $\mathcal{E}_{12,3} = \{(54, 19), (54, 27), (54, 55), (54, 35)\} \subset \mathcal{E}$, and $\mathcal{E}_{12,4} = \{(46, 19), (46, 55), (46, 35), (46, 27)\} \subset \mathcal{E}$. The four possible movement phases at junction 12 are shown in Fig. 2.

Assumption 1. The next movement phase at junction $i \in \mathcal{V}$ can be either the same as or different with the current movement phase. Mathematically, The next movement phase $\mathcal{E}_{i,h}$ is not necessarily different with the current movement phase $\mathcal{E}_{i,l}$, if $(\mathcal{E}_{i,l}, \mathcal{E}_{i,h}) \in \mathcal{R}_i$.

Assumption 1 implies that the phase rotation cycle is still advanced, if next movement phase $\mathcal{E}_{i,h}$ is either the same as or different with current movement phase $\mathcal{E}_{i,l}$,

Assumption 2. Movement phase rotation occurs concurrently across the NOIR junctions.

Assumption 2 is not a restricting assumption since repetition of movement phases is authorized at a junction per Assumption 1. Indeed the duration of particular movement phase $\mathcal{E}_{i,j}$ ($j = 1, \dots, r_i$) can be chosen arbitrarily large through defining edge set \mathcal{R}_i for $i \in \mathcal{W}$. As shown in Fig. 3, repetition of a particular movement phase denoted by $\mathcal{E}_{i,j}$, is authorized by defining $\mathcal{E}_{i,k} = \mathcal{E}_{i,j}$ and $\mathcal{E}_{i,l} = \mathcal{E}_{i,j}$ where $(\mathcal{E}_{i,j}, \mathcal{E}_{i,k}) \in \mathcal{R}_i$ and $(\mathcal{E}_{i,k}, \mathcal{E}_{i,l}) \in \mathcal{R}_i$.

Definition 1. The NOIR movement phase rotation is cyclic and defined by graph $C_{\text{NOIR}}(\mathcal{L}, \mathcal{M})$ with node set

$$\mathcal{L} = \mathcal{E}_1 \times \dots \times \mathcal{E}_m$$

and edge set $\mathcal{M} \subset \mathcal{L} \times \mathcal{L}$, where \times is the Cartesian product symbol.

Theorem 1. Let r_i be the number of movement phases at junction $i \in \mathcal{W} = \{1, \dots, m\}$, and movement phase rotation be cyclic and satisfy condition 4 at every junction $i \in \mathcal{W} =$

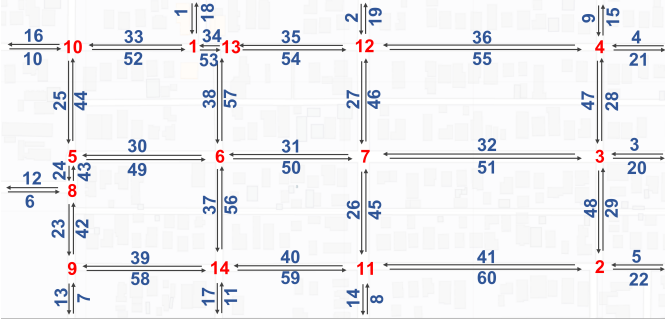


Fig. 1: Example NOIR: Street map of Phoenix. Numbers in blue denote the unidirectional roads $\mathcal{V} = \{1, \dots, 60\}$, and red color numbers represent junctions $\mathcal{W} = \{1, \dots, 14\}$.

$\{1, \dots, m\}$. Then, the NOIR cycle is completed in n_c time steps where

$$n_c = \text{lcm}(r_1, \dots, r_m) \quad (3)$$

is the lowest common multiple of r_1, \dots, r_m .

Proof. Completion of movement phase rotation at every junction is deterministic and independent of other junctions at every junction $i \in \mathcal{W}$. By imposing Assumption 2, The edges of graph $C_{\text{NOIR}}(\mathcal{L}, \mathcal{M})$, defined by \mathcal{L} , are restricted to satisfy the following constraints:

$$\bigwedge_{i \in \mathcal{W}} \bigwedge_{j=1}^{r_i} \bigwedge_{h=1}^{r_i} ((\mathcal{E}_{i,j}, \mathcal{E}_{i,h}) \in \mathcal{R}_i). \quad (4)$$

Because movement phase rotation, completed in r_i time steps, is independent at every junction $i \in \mathcal{W}$, the cycle of graph C_{NOIR} is completed in n_c time steps where n_c is the lowest common multiple of r_1, \dots, r_m and obtained by (4). \square

Per Theorem 1, graph $C_{\text{NOIR}}(\mathcal{L}, \mathcal{M})$ consists of n_c nodes defined by set

$$\mathcal{L} = \{\lambda_j = (\mathcal{E}_{1,j}, \dots, \mathcal{E}_{i,j}, \mathcal{E}_{m,j}) : i \in \mathcal{W}, j = 0, 1, \dots, n_c - 1\} \quad (5)$$

Definition 2. The identification number of the NOIR movement phases are defined by set

$$\sigma = \{0, \dots, n_c - 1\}. \quad (6)$$

Fig. 4 shows an example graph C_{NOIR} specifying the NOIR movement phase rotations for a traffic network with m junctions.

III. PROBLEM STATEMENT

Before proceeding to state the problem studied in this paper, we define variables $\zeta[k] \in \sigma$ and $\gamma[k] \in \sigma$ by

$$\begin{aligned} \zeta[k] &= k \bmod n_c \\ \gamma[k] &= (k+1) \bmod n_c = \zeta[k] + 1 \bmod n_c \end{aligned}$$

We apply the cell transmission model to model traffic in a NOIR by

$$\rho_i[k+1] = \rho_i[k] + y_i[k] - z_i[k] + u_i[k], \quad (7)$$

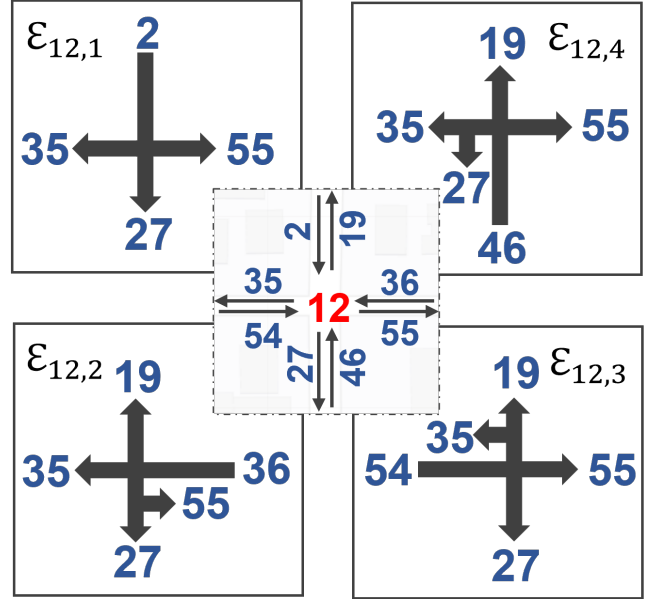


Fig. 2: Possible movement phases at junction $12 \in \mathcal{W}$

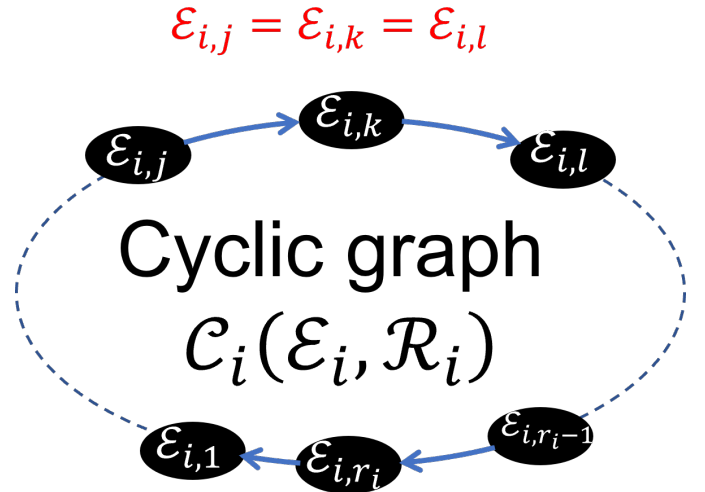


Fig. 3: Example NOIR: Street map of Phoenix

where ρ_i is the traffic density; u_i is the boundary inflow; and z_i and y_i are the network outflow and network inflow of road $i \in \mathcal{V}$, respectively; and they are defined as follows:

$$z_i[k] = p_{i, \lambda_{\zeta[k]}} \rho_i[k], \quad \lambda_{\zeta[k]} \in \mathcal{L}, \zeta[k] \in \sigma \quad (8a)$$

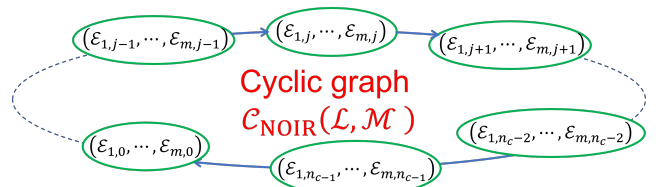


Fig. 4: Schematic of the cyclic graph C_i with movement phase repetition.

$$\begin{aligned}
y_i[k] &= \sum_{j \in \mathcal{O}_i} q_{j,i,\lambda_\zeta[k]} z_j[k] \\
&= \sum_{j \in \mathcal{O}_i} q_{j,i,\lambda_\zeta[k]} p_{j,\lambda_\zeta[k]} \rho_j[k], \quad \lambda_\zeta[k] \in \mathcal{L}, \zeta[k] \in \sigma
\end{aligned} \tag{8b}$$

at every discrete time k . Note that

$$(\lambda_\zeta[k], \lambda_\gamma[k]) \in \mathcal{M}, \quad \forall k, \tag{9}$$

where $p_{i,\lambda_\zeta[k]} \in (0, 1]$ is the outflow probability of road $i \in \mathcal{V}$ at discrete time k when $\lambda_\zeta[k] \in \mathcal{M}$ is the active NOIR movement phase. Also, $q_{j,i,\lambda_\zeta[k]} \in (0, 1]$ assigns the fraction of outflow of road $i \in \mathcal{V}$ directed towards $j \in \mathcal{O}_i$ under NOIR movement phase $\lambda_\zeta[k] \in \mathcal{M}$ at discrete time k .

To assure the traffic feasibility, traffic density of road $i \in \mathcal{V}$ must satisfy the following inequality constraints:

$$\bigwedge_{i \in \mathcal{V}_{in}} (u_i[k] \geq 0), \quad k \in \mathbb{N}, \tag{10a}$$

$$\sum_{i \in \mathcal{V}_{in}} u_i[k] = u_0, \quad k \in \mathbb{N}, \tag{10b}$$

$$\bigwedge_{i \in \mathcal{V}} (0 \leq \rho_i[k] \leq \bar{\rho}_{\max}), \quad k \in \mathbb{N}. \tag{10c}$$

Condition (10a) ensures that the boundary inflow is non-negative at every discrete time k . Condition (10b), requiring the net boundary inflow is equal to constant value u_0 , is valid when the demand for using the NOIR is high. Condition (10c) assures that the traffic density is always positive and does not exceed ρ_{\max} . We use the Fundamental Diagram (FD) [27] with the schematic shown in Fig. 5 to assure feasibility of the network outflow at every road $i \in \mathcal{V}$. As shown in Fig. 5, the fundamental diagram is a trapezoid that is determined by knowing $\bar{\rho}_{\min}$, $\bar{\rho}_{\text{mid}}$, $\bar{\rho}_{\max}$, and \bar{z}_{\max} . In particular, the FD is applied to assure that the outflow of road $i \in \mathcal{V}$, denoted by z_i is feasible by satisfying the following inequality constraints:

$$\bigwedge_{i \in \mathcal{V}} (z_i[k] \geq 0), \quad k \in \mathbb{N}, \tag{11a}$$

$$\bigwedge_{i \in \mathcal{V}} \left(z_i[k] \leq \frac{\bar{z}_{\max} \rho_i[k]}{\bar{\rho}_{\min}} \right), \quad k \in \mathbb{N}, \tag{11b}$$

$$\bigwedge_{i \in \mathcal{V}} (z_i[k] \leq \bar{z}_{\max}), \quad k \in \mathbb{N}, \tag{11c}$$

$$\bigwedge_{i \in \mathcal{V}} \left(z_i[k] \leq \frac{\bar{z}_{\max} (\rho_i[k] - \bar{\rho}_{\max})}{(\bar{\rho}_{\text{mid}} - \bar{\rho}_{\max})} \right), \quad k \in \mathbb{N}. \tag{11d}$$

The objective of this paper is to determine boundary inflow $u_i[k]$ at every road $i \in \mathcal{V}$ and every discrete time k such that the traffic coordination cost defined by

$$J = \sum_{j=1}^{n_c} \left(\sum_{i \in \mathcal{V}_{in}} u_i^2[k+j] + \beta \sum_{i \in \mathcal{V}} \rho_i^2[k+j] \right) \tag{12}$$

is minimized, where scaling parameter $\beta > 0$ is constant.

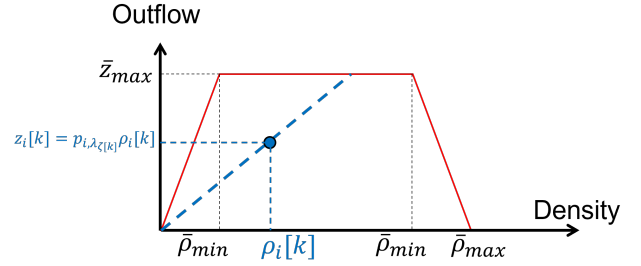


Fig. 5: Graphic representation of constraint equation (11) imposed by the trapezoid fundamental diagram [27]. The left limit of the diagram corresponds to constraint (11b); the top limit to constraint (11c); and the right limit to constraint (11d).

IV. PROBLEM SPECIFICATION

We can express the requirements from Section III in Linear Temporal Logic (LTL). Every LTL formula consists of a set of atomic propositions, logical operators, and temporal operators. Logical operators include \neg (“negation”), \vee (“disjunction”), \wedge (“conjunction”), and \Rightarrow (“implication”). LTL formulae also use temporal operators \square (“always”), \bigcirc (“next”), \diamond (“eventually”), and \mathcal{U} (“until”).

The traffic evolution governed by (7) must satisfy the feasibility requirements (equations (10a)-(10c)), leading to the requirements:

$$\bigwedge_{i \in \mathcal{V}_{in}} \square (u_i \geq 0), \tag{13a}$$

$$\square \left(\sum_{i \in \mathcal{V}_{in}} u_i = u_0 \right), \tag{13b}$$

$$\bigwedge_{i \in \mathcal{V}} \square (\rho_i \geq 0), \tag{13c}$$

$$\bigwedge_{i \in \mathcal{V}} \square (\rho_i \leq \bar{\rho}_{\max}). \tag{13d}$$

Additionally the movement phase rotation can be expressed as:

$$\square ((\lambda_\zeta, \lambda_\gamma) \in \mathcal{M}). \tag{14}$$

We can also concisely express the FD constraints (Eq. (9) and Eqs. (11a)-(11d)), leading to the LTL requirements:

$$\bigwedge_{i \in \mathcal{V}} \square (z_i \geq 0), \tag{15a}$$

$$\bigwedge_{i \in \mathcal{V}} \square \left(z_i \leq \frac{\bar{z}_{\max} \rho_i}{\bar{\rho}_{\min}} \right), \tag{15b}$$

$$\bigwedge_{i \in \mathcal{V}} \square (z_i \leq \bar{z}_{\max}), \tag{15c}$$

$$\bigwedge_{i \in \mathcal{V}} \square \left(z_i \leq \frac{\bar{z}_{\max} (\rho_i - \bar{\rho}_{\max})}{(\bar{\rho}_{\text{mid}} - \bar{\rho}_{\max})} \right). \tag{15d}$$

The objective of traffic congestion control is to satisfy the following liveness conditions:

$$\diamond \left(\left| \bigwedge_{i \in \mathcal{V}_{out}} z_i - u_0 \right| < \epsilon \right), \tag{16}$$

where ϵ is constant and obtained in Section V. Liveness condition (25) specifies the reachability of the traffic state to the steady-state condition where the network inflow and outflow are the same. Theorem 3 presented in Section V proves that the liveness condition (25) is satisfied if the proposed first order dynamics is used to model the traffic coordination.

V. TRAFFIC NETWORK DYNAMICS

To obtain the traffic network dynamics, we define tendency probability matrix $\mathbf{Q}(\zeta[k]) = [q_{i,j,\zeta[k]}] \in \mathbb{R}^{N \times N}$, outflow probability matrix

$$\mathbf{P}(\zeta[k]) = \text{diag}\left(p_{1,\lambda_\zeta[k]}, \dots, p_{N,\lambda_\zeta[k]}\right) \in \mathbb{R}^{N \times N}, \quad \lambda \in \mathcal{L}, \quad (17)$$

and

$$\mathbf{A}(\zeta[k]) = \mathbf{I} + (\mathbf{Q}(\zeta[k]) - \mathbf{I})\mathbf{P}(\zeta[k]), \quad \zeta \in \sigma, k \in \mathbb{N}. \quad (18)$$

We also define matrix $\mathbf{B} = [b_{ij}] \in \mathbb{R}^{N \times N}$ with the (i, j) entry that is defined as follows:

$$b_{ij} = \begin{cases} 1 & i \in \mathcal{I}_j \\ 0 & \text{otherwise} \end{cases}. \quad (19)$$

By defining the state vector $\mathbf{x}[k] = [\rho_1[k] \ \dots \ \rho_N[k]]^\top$ and input vector $\mathbf{u}[k] = [u_1[k] \ \dots \ u_{N_{in}}[k]]^\top$, and imposing the CTM given in (7), the traffic network dynamics is obtained as follows:

$$\mathbf{x}[k+1] = \mathbf{A}(\zeta[k])\mathbf{x}[k] + \mathbf{B}\mathbf{u}[k], \quad \zeta \in \sigma. \quad (20)$$

Given the above definitions, matrices $\mathbf{P}(\zeta[k])$ and $\mathbf{Q}(\zeta[k])$ hold the following properties:

Property 3. *Entries of the diagonal matrix $\mathbf{P}(\zeta[k])$ are positive and not greater than 1 because $p_{i,\lambda_\zeta[k]} \in (0, 1]$ for every $i \in \mathcal{V}$.*

Property 4. *Matrix $\mathbf{Q}(\zeta[k])$ is a non-negative matrix because $q_{j,i,\lambda_\zeta[k]} \in (0, 1]$ for every $i \in \mathcal{V}$.*

Property 5. *Diagonal entries of matrix $\mathbf{Q}(\zeta[k])$ are 0 because $i \notin \mathcal{O}_i$ for every $i \in \mathcal{V}$.*

Property 6. *Because road elements in the NOIR are unidirectional interconnected, graph $\mathcal{G}(\mathcal{V}, \mathcal{E})$ holds the property that:*

$$(i, j) \in \mathcal{E} \implies (j, i) \notin \mathcal{E}, \quad \forall i, j \in \mathcal{V},$$

which indicates that off-diagonal entries of matrix $\mathbf{Q}(\zeta[k])$ follow the relation that:

$$Q_{i,j,\lambda_\zeta[k]} \neq 0 \implies Q_{j,i,\lambda_\zeta[k]} = 0, \quad \forall i \neq j \cap i, j \in \mathcal{V}.$$

Property 7. *At each discrete time $k \in \mathbb{N}$,*

$$\sum_{j=1}^N Q_{j,i,\lambda_\zeta[k]} = 0, \quad \forall i \in \mathcal{V}_{out} \quad (21a)$$

$$\sum_{j \in \mathcal{O}_i} q_{j,i,\lambda_\zeta[k]} = \sum_{j=1}^N Q_{j,i,\lambda_\zeta[k]} = 1, \quad \forall i \in \mathcal{V} \setminus \mathcal{V}_{out} \quad (21b)$$

Theorem 2. *If Properties 3-7 are all satisfied at each discrete time k , the traffic dynamics (20) is BIBO stable.*

Proof: According to the Gershgorin circle theorem [28], every eigenvalue of matrix $\mathbf{Q}(\zeta[k]) - \mathbf{I}$ lies within at least one of the Gershgorin discs $D(-1, 1)$. Because entries of matrix $\mathbf{P}(\zeta[k])$ are all in the interval $(0, 1]$, eigenvalues of matrix $\mathbf{A}(\zeta[k])$ must be located within the discs $D(0, 1)$ [29]. If this is not satisfied and some of the eigenvalues of $\mathbf{A}(\zeta[k])$ are 1, then, 0 is an element of the spectrum of matrix $\mathbf{Q}(\zeta[k]) - \mathbf{I}$, which indicates that the matrix $\mathbf{Q}(\zeta[k]) - \mathbf{I}$ is not full rank, i.e. $\text{rank}(\mathbf{Q}(\zeta[k]) - \mathbf{I}) < N$. However, considering the properties 5 and 6 of matrix \mathbf{Q} , it can be seen that rows of matrix $\mathbf{Q}(\zeta[k]) - \mathbf{I}$ are independent, which implies that the rank of matrix $\text{rank}(\mathbf{Q}(\zeta[k]) - \mathbf{I}) = N$. Therefore, since the assumption of matrix $\mathbf{A}(\zeta[k])$ can not be satisfied, we can draw the conclusion that eigenvalues of matrix \mathbf{A} must be located within the discs $D(0, 1)$ strictly, i.e. the spectral radius $\rho(\mathbf{A}(\zeta[k])) < 1$. Then, since eigenvalues of matrix $\mathbf{A}(\zeta[k])$ are within the unit circle strictly at each discrete time k , the traffic dynamics (20) is BIBO stable [10], [30].

Theorem 3. *If Properties 3-7 of matrices $\mathbf{P}(\zeta[k])$ and $\mathbf{Q}(\zeta[k])$ are all satisfied, then, liveness condition (25) is satisfied.*

Proof. The traffic dynamics (20) can be rewritten as

$$\mathbf{x}[k+1] = \mathbf{x}[k] + (\mathbf{Q}(\zeta[k]) - \mathbf{I})\mathbf{z}[k] + \mathbf{B}\mathbf{u}[k], \quad \zeta \in \sigma, k \in \mathbb{N}. \quad (22)$$

Therefore,

$$\mathbf{1}_{1 \times N} (\mathbf{x}[k+1] - \mathbf{x}[k]) = \mathbf{1}_{1 \times N} (\mathbf{Q}(\zeta[k]) - \mathbf{I})\mathbf{z}[k] + u_0, \quad \zeta \in \sigma. \quad (23)$$

where $\mathbf{1}_{1 \times N} \in \mathbb{R}^{1 \times N}$ is a row vector, with entries that are all 1, $u_0 = \mathbf{1}_{1 \times N} \mathbf{B}\mathbf{u}[k]$ is constant at every discrete time k per condition (10b). Because traffic dynamics (20) is BIBO stable, there exists a discrete time k_s such that

$$|\mathbf{1}_{1 \times N} (\mathbf{x}[k+1] - \mathbf{x}[k])| < \delta_1, \quad \forall k \geq k_s, \quad (24a)$$

$$\left| \mathbf{1}_{1 \times N} (\mathbf{Q}(\zeta[k]) - \mathbf{I})\mathbf{z}[k] - \sum_{i \in \mathcal{V}_{out}} z_i[k] \right| < \delta_2, \quad \forall k \geq k_s. \quad (24b)$$

Note the $z_i[k] > 0$ at every time k , therefore,

$$\left| \bigwedge_{i \in \mathcal{V}_{out}} z_i[k] - u_0 \right| < \epsilon = \delta_1 + \delta_2 \quad \forall k \geq k_s. \quad (25)$$

□

VI. TRAFFIC CONGESTION CONTROL

We use MPC to determine the boundary control $\mathbf{u}[k]$ at every discrete time k by solving a quadratic programming problem with a quadratic cost and linear constraints imposing the feasibility conditions into management of traffic coordination. To this end, we first define matrix multiplication process

$$\mathbf{H}(\zeta[k+i]) = \mathbf{H}(\zeta[k+i-1])\mathbf{A}(\zeta[k]), \quad i \in \sigma. \quad (26)$$

subject to

$$\mathbf{H}(\zeta[k]) = \mathbf{I}. \quad (27)$$

We then apply (20) to predict the traffic evolution within the next n_c sampling times by

$$\mathbf{X}[k] = \mathbf{G}_1(\zeta[k])\mathbf{x}[k] + \mathbf{G}_2(\zeta[k])\mathbf{U}[k], \quad k \in \mathbb{N}, \zeta \in \sigma \quad (28)$$

$$\mathbf{G}_1(\zeta[k]) = \begin{bmatrix} \mathbf{H}(\zeta[k+1]) \\ \vdots \\ \mathbf{H}(\zeta[k+n_c]) \end{bmatrix} \in \mathbb{R}^{N n_c \times N}, \quad k \in \mathbb{N}, \zeta \in \sigma, \quad (29a)$$

$$\mathbf{G}_2(\zeta[k]) = \begin{bmatrix} \mathbf{H}(\zeta[k]) & \mathbf{0} & \mathbf{0} & \cdots & \mathbf{0} \\ \mathbf{H}(\zeta[k+1]) & \mathbf{H}(\zeta[k]) & \mathbf{0} & \cdots & \mathbf{0} \\ \mathbf{H}(\zeta[k+2]) & \mathbf{H}(\zeta[k+1]) & \mathbf{H}(\zeta[k]) & \cdots & \mathbf{0} \\ \vdots & \vdots & \vdots & \ddots & \vdots \\ \mathbf{H}(\zeta[k+n_c-1]) & \mathbf{H}(\zeta[k+n_c-2]) & \mathbf{H}(\zeta[k+n_c-3]) & \cdots & \mathbf{H}(\zeta[k]) \end{bmatrix} (\mathbf{B} \otimes \mathbf{1}_{1 \times n_c}) \in \mathbb{R}^{N n_c \times N n_c}, \quad k \in \mathbb{N}, \zeta \in \sigma \quad (29b)$$

In Eq. (29b) \otimes is the Kronecker product symbol and $\mathbf{1}_{1 \times n_c} \in \mathbb{R}^{1 \times n_c}$ is a row vector with the entries that are all 1.

The cost function J , previously defined in (12), can be rewritten as follows:

$$J(\mathbf{U}[k], \zeta[k]) = \frac{1}{2} \mathbf{U}^\top[k] \mathbf{W}_1(\zeta[k]) \mathbf{U}[k] + \mathbf{W}_2^\top(\zeta[k]) \mathbf{U}[k] + \mathbf{W}_3(\zeta[k]), \quad (30)$$

where

$$\mathbf{W}_1(\zeta[k]) = \mathbf{I} + \beta \mathbf{G}_2^\top(\zeta[k]) \mathbf{G}_2(\zeta[k]), \quad (31a)$$

$$\mathbf{W}_2^\top(\zeta[k]) = \beta \mathbf{x}^\top[k] \mathbf{G}_1^\top(\zeta[k]) \mathbf{G}_2(\zeta[k]), \quad (31b)$$

$$\mathbf{W}_3(\zeta[k]) = \frac{1}{2} \beta \mathbf{x}^\top[k] \mathbf{G}_1^\top(\zeta[k]) \mathbf{G}_1(\zeta[k]) \mathbf{x}[k]. \quad (31c)$$

Note that $\mathbf{W}_3(\zeta[k])$ can be removed from cost function (30) because it does not depend on $\mathbf{U}[k]$ at every discrete time k . Therefore,

$$J' = \frac{1}{2} \mathbf{U}^\top[k] \mathbf{W}_1(\zeta[k]) \mathbf{U}[k] + \mathbf{W}_2^\top(\zeta[k]) \mathbf{U}[k] \quad (32)$$

is considered as the cost function of traffic coordination, and the optimal control variable

$$\mathbf{u}^*[k] = [\mathbf{I}_{N_{in}} \quad \mathbf{0}_{N_{in} \times N_{in}(N_c-1)}] \mathbf{U}^*[k] \quad (33)$$

is assigned by determining $\mathbf{U}^*[k]$ by solving of the following optimization problem:

$$\min J' = \min \left(\frac{1}{2} \mathbf{U}^\top[k] \mathbf{W}_1(\zeta[k]) \mathbf{U}[k] + \mathbf{W}_2^\top(\zeta[k]) \mathbf{U}[k] \right)$$

subject to

$$-\mathbf{G}_2(\zeta[k]) \mathbf{U}[k] \leq \mathbf{G}_1(\zeta[k]) \mathbf{x}[k], \quad (34a)$$

$$\mathbf{G}_2(\zeta[k]) \mathbf{U}[k] \leq -\mathbf{G}_1(\zeta[k]) \mathbf{x}[k] + \bar{\rho}_{max} \mathbf{1}_{N n_c \times 1}, \quad (34b)$$

$$\left(\mathbf{W}_4(\zeta[k]) - \frac{\bar{\zeta}_{max}}{\bar{\rho}_{min}} \mathbf{I} \right) \mathbf{G}_2(\zeta[k]) \mathbf{U}[k] \leq -\mathbf{G}_1(\zeta[k]) \mathbf{x}[k], \quad (34c)$$

$$\mathbf{W}_4(\zeta[k]) \mathbf{G}_2(\zeta[k]) \mathbf{U}[k] \leq -\mathbf{G}_1(\zeta[k]) \mathbf{x}[k] + \mathbf{v}_1, \quad (34d)$$

where $\mathbf{X}[k] = [\mathbf{x}^\top[k+1] \cdots \mathbf{x}^\top[k+n_c]]^\top$, $\mathbf{U}[k] = [\mathbf{u}^\top[k] \cdots \mathbf{u}^\top[k+n_c-1]]^\top$, and matrices $\mathbf{G}_1(\zeta[k])$ and $\mathbf{G}_2(\zeta[k])$ are defined by (29a) and (29b), respectively.

ID	Name	Direction	ID	Name	Direction
1	N10th St.(E McKinley St.- E Pierce St.)	S	2	N11th St.(E McKinley St.- E Pierce St.)	S
3	E Fillmore St.(N12th St.- N13th St.)	W	4	E Pierce St.(N12th St.- N13th St.)	W
5	E Taylor St.(N12th St.- N13th St.)	W	6	E Fillmore St.(N7th St.- N9th St.)	E
7	N9th St.(E Taylor St.- E Polk St.)	N	8	N11th St.(E Taylor St.- E Polk St.)	N
9	N12th St.(E McKinley St.- E Pierce St.)	S	10	E Pierce St.(N7th St.- N9th St.)	E
11	N10th St.(E Taylor St.- E Polk St.)	N	12	E Fillmore St.(N7th St.- N9th St.)	W
13	N9th St.(E Taylor St.- E Polk St.)	S	14	N11th St.(E Taylor St.- E Polk St.)	S
15	N12th St.(E McKinley St.- E Pierce St.)	N	16	E Pierce St.(N7th St.- N9th St.)	W
17	N10th St.(E Taylor St.- E Polk St.)	S	18	N10th St.(E McKinley St.- E Pierce St.)	N
19	N11th St.(E McKinley St.- E Pierce St.)	N	20	E Fillmore St.(N12th St.- N13th St.)	E
21	E Pierce St.(N12th St.- N13th St.)	E	22	E Taylor St.(N12th St.- N13th St.)	E
23	N9th St.(E Fillmore St.- E Taylor St.)	S	24	N9th St.(E Fillmore St.- E Taylor St.)	S
25	N9th St.(E Pierce St.- E Fillmore St.)	S	26	N11th St.(E Fillmore St.- E Taylor St.)	S
27	N11th St.(E Pierce St.- E Fillmore St.)	S	28	N12th St.(E Pierce St.- E Fillmore St.)	N
29	N12th St.(E Fillmore St.- E Taylor St.)	N	30	E Fillmore St.(N9th St.- N10th St.)	W
31	E Fillmore St.(N10th St.- N11th St.)	W	32	E Fillmore St.(N11th St.- N12th St.)	W
33	E Pierce St.(N9th St.- N10th St.)	W	34	E Pierce St.(N10th St.- N11th St.)	W
35	E Pierce St.(N10th St.- N11th St.)	W	36	E Pierce St.(N11th St.- N12th St.)	W
37	N10th St.(E Fillmore St.- E Taylor St.)	S	38	N10th St.(E Pierce St.- E Fillmore St.)	S
39	E Taylor St.(N9th St.- N10th St.)	W	40	E Taylor St.(N10th St.- N11th St.)	W
41	E Taylor St.(N11th St.- N12th St.)	W	42	N9th St.(E Fillmore St.- E Taylor St.)	N
43	N9th St.(E Fillmore St.- E Taylor St.)	N	44	N9th St.(E Pierce St.- E Fillmore St.)	N
45	N11th St.(E Fillmore St.- E Taylor St.)	N	46	N11th St.(E Pierce St.- E Fillmore St.)	N
47	N12th St.(E Pierce St.- E Fillmore St.)	S	48	N12th St.(E Fillmore St.- E Taylor St.)	S
49	E Fillmore St.(N9th St.- N10th St.)	E	50	E Fillmore St.(N10th St.- N11th St.)	E
51	E Fillmore St.(N11th St.- N12th St.)	E	52	E Pierce St.(N9th St.- N10th St.)	E
53	E Pierce St.(N10th St.- N11th St.)	E	54	E Pierce St.(N10th St.- N11th St.)	E
55	E Pierce St.(N11th St.- N12th St.)	E	56	N10th St.(E Fillmore St.- E Taylor St.)	N
57	N10th St.(E Pierce St.- E Fillmore St.)	N	58	E Taylor St.(N9th St.- N10th St.)	E
59	E Taylor St.(N10th St.- N11th St.)	E	60	E Taylor St.(N11th St.- N12th St.)	E

TABLE I: Road elements of the example NOIR of Phoenix City

$$\left(\mathbf{W}_4(\zeta[k]) + \frac{\bar{\zeta}_{max}}{\bar{\rho}_{max} - \bar{\rho}_{mid}} \mathbf{I} \right) (\zeta[k]) \mathbf{G}_2(\zeta[k]) \mathbf{U}[k] \leq \quad (34e)$$

$$-\mathbf{G}_1(\zeta[k]) \mathbf{x}[k] + \mathbf{v}_2,$$

$$\mathbf{I}_{n_c} \otimes \mathbf{1}_{1 \times N_{in}} \mathbf{U}[k] = -u_0 \mathbf{1}_{n_c \times 1}, \quad (34f)$$

where

$$\mathbf{W}_4(\zeta[k]) = \begin{bmatrix} \mathbf{P}(\zeta[k+1]) & \cdots & \mathbf{0} \\ \vdots & \ddots & \vdots \\ \mathbf{0} & \cdots & \mathbf{P}(\zeta[k+n_c]) \end{bmatrix} \in \mathbb{R}^{N n_c \times N n_c}, \quad (35a)$$

$$\mathbf{v}_1 = \bar{\zeta}_{max} \mathbf{1}_{N n_c}, \quad (35b)$$

$$\mathbf{v}_2 = \frac{\bar{\zeta}_{max} \bar{\rho}_{max}}{\bar{\rho}_{max} - \bar{\rho}_{mid}} \mathbf{1}_{N n_c}. \quad (35c)$$

VII. SIMULATION RESULTS

We simulate traffic congestion control in a selected area in Downtown Phoenix with the map and NOIR shown in Fig. 1. The NOIR consisting of 60 unidirectional roads with the

TABLE II: Number of movement phases at every junction $i \in \mathcal{W}$

Number of movement phases at junction i denoted by r_i													
r_1	r_2	r_3	r_4	r_5	r_6	r_7	r_8	r_9	r_{10}	r_{11}	r_{12}	r_{13}	r_{14}
3	3	4	4	3	4	4	3	3	3	4	4	3	4

TABLE III: Active incoming roads at junctions defined by \mathcal{W} over the entire cycle of length $n_c = 12$

$i \in \mathcal{W}$	Active movement phases over a cycle											
	$k+1$	$k+2$	$k+3$	$k+4$	$k+5$	$k+6$	$k+7$	$k+8$	$k+9$	$k+10$	$k+11$	$k+12$
1	1	34	52	1	34	52	1	34	52	1	34	52
2	48	5	60	48	5	60	48	5	60	48	5	60
3	47	3	29	51	47	3	29	51	47	3	29	51
4	9	4	28	55	9	4	28	55	9	4	28	55
5	25	30	43	25	30	43	25	30	43	25	30	43
6	38	31	56	49	38	31	56	49	38	31	56	49
7	27	32	45	50	27	32	45	50	27	32	45	50
8	24	42	6	24	42	6	24	42	6	24	42	6
9	23	39	7	23	39	7	23	39	7	23	39	7
10	33	44	10	33	44	10	33	44	10	33	44	10
11	26	41	8	59	26	41	8	59	26	41	8	59
12	2	36	46	54	2	36	46	54	2	36	46	54
13	35	57	53	35	57	53	35	57	53	35	57	53
14	37	40	11	58	37	40	11	58	37	40	11	58

identification numbers defined by set $\mathcal{V} = \{1, \dots, 60\}$ and the names listed in Table I. Interconnections between roads are defined by $\mathcal{G}(\mathcal{V}, \mathcal{E})$ with node set \mathcal{V} and edge set \mathcal{E} , where $\mathcal{V} = \mathcal{V}_{in} \cup \mathcal{V}_{out} \cup \mathcal{V}_I$, $\mathcal{V}_{in} = \{1, \dots, 11\}$, $\mathcal{V}_I = \{12, \dots, 22\}$. As shown in Fig. 1, the NOIR consists of 14 junctions defined by set $\mathcal{W} = \{1, \dots, 14\}$. Without loss of generality, for definition of movement phases, we make the following assumption in addition to Assumptions 1 and 2:

Assumption 3. *At every discrete time $k \in \mathbb{N}$, traffic can enter junction $i \in \mathcal{W}$ through a single incoming road which is called active incoming road.*

By imposing Assumption 3, the number of movement phases is either 3 or 4 at every junction $i \in \mathcal{W}$ (see Table II). Therefore, the NOIR cycle is completed in $n_c = 12$ time steps. Table III lists the active incoming roads over the NOIR cycle of the length $n_c = 12$.

For traffic simulation, we consider the same FD to obtain traffic feasibility conditions at every road $i \in \mathcal{W}$ and choose the simulation parameters listed in Table IV. The optimal boundary inflow is plotted versus discrete time k in Fig. 6 for $k = 1, \dots, 60$. Fig. 7 shows the outflow of z_i of every road $i \in \mathcal{V}$ at sample times $k = 15$, $k = 30$, and $k = 50$. It is seen that the feasibility conditions imposed by the FD are all satisfied. Also, the net traffic density ($\sum_{i \in \mathcal{V}} \rho_i$) versus discrete time k is plotted in Fig. 8.

VIII. CONCLUSION

In this paper, we introduced a new physics-inspired approach law to model the traffic evolution and control congestion through the boundary roads of a NOIR. By commanding cyclic movement phase rotation at NOIR junctions, we modeled traffic coordination by a switching discrete time dynamics, with deterministic transitions over finite states representing NOIR movement phases. We used a trapezoid FD to formally

TABLE IV: Simulation parameters for every $i \in \mathcal{V}$

$\bar{z}_{i,max}$	$\bar{\rho}_{i,min}$	$\bar{\rho}_{i,mid}$	$\bar{\rho}_{i,max}$	u_0
20	20	40	55	50

specify the feasibility and liveness conditions for traffic coordination. The feasibility conditions impose linear equality and inequality constraints on traffic congestion control, which was defined as a receding horizon optimization problem, and can be solved as a quadratic programming problem.

REFERENCES

- [1] T. Reed, "Inrix global traffic scorecard," Feb. 2019.
- [2] C. F. Daganzo, "The cell transmission model, part ii: Network traffic," *Transportation Research Part B: Methodological*, vol. 29, no. 2, pp. 79–93, 1995.
- [3] Q. Ba and K. Savla, "On distributed computation of optimal control of traffic flow over networks," in *54th Annual Allerton Conference on Communication, Control, and Computing*. IEEE, 2016, pp. 1102–1109.
- [4] N. Geroliminis and C. F. Daganzo, "Existence of urban-scale macroscopic fundamental diagrams: Some experimental findings," *Transportation Research Part B: Methodological*, vol. 42, no. 9, pp. 759–770, 2008.
- [5] L. Munoz, X. Sun, R. Horowitz, and L. Alvarez-Icaza, "Traffic density estimation with the cell transmission model," vol. 5, 07 2003, pp. 3750 – 3755.
- [6] L. Yang, S. Yin, K. Han, J. Haddad, and M. Hu, "Fundamental diagrams of airport surface traffic: Models and applications," *Transportation Research Part B: Methodological*, vol. 106, pp. 29–51, 2017.
- [7] N. Geroliminis, J. Haddad, and M. Ramezani, "Optimal perimeter control for two urban regions with macroscopic fundamental diagrams: A model predictive approach," *Intelligent Transportation Systems, IEEE Transactions on*, vol. 14, pp. 348–359, 03 2013.
- [8] J. Haddad, "Optimal perimeter control synthesis for two urban regions with aggregate boundary queue dynamics," *Transportation Research Part B: Methodological*, vol. 96, pp. 1–25, 2017.
- [9] S. Li, W. Zhu, and X. Dong, "Traffic flow feedback control strategy based on macroscopic fundamental diagram," in *2017 Chinese Automation Congress (CAC)*, 2017, pp. 2508–2512.
- [10] X. Liu and H. Rastgoftar, "Conservation-based modeling and boundary control of congestion with an application to traffic management in center city philadelphia," *2021 Australian & New Zealand Control Conference (ANZCC)*, pp. 49–54, 2021.
- [11] A. Jamshidnejad, I. Papamichail, M. Papageorgiou, and B. De Schutter, "Sustainable model-predictive control in urban traffic networks: Efficient solution based on general smoothing methods," *IEEE Transactions on Control Systems Technology*, vol. 26, no. 3, pp. 813–827, 2018.
- [12] H. Rastgoftar, J.-B. Jeannin, and E. Atkins, "An integrative behavioral-based physics-inspired approach to traffic congestion control," ser. Dynamic Systems and Control Conference, vol. 2, 10 2020, v002T23A003. [Online]. Available: <https://doi.org/10.1115/DSCC2020-3330>
- [13] S. Lin, B. De Schutter, Y. Xi, and H. Hellendoorn, "Fast model predictive control for urban road networks via milp," *IEEE Transactions on Intelligent Transportation Systems*, vol. 12, pp. 846 – 856, 10 2011.
- [14] S. Chiu and S. Chand, "Adaptive traffic signal control using fuzzy logic," in *Second IEEE International Conference on Fuzzy Systems*, 1993, pp. 1371–1376 vol.2.
- [15] W. Wei, Y. Zhang, J. Mbede, Z. Zhang, and J. Song, "Traffic signal control using fuzzy logic and moga," in *2001 IEEE International Conference on Systems, Man and Cybernetics*, vol. 2, 2001, pp. 1335–1340 vol.2.
- [16] J. J. Sanchez-Medina, M. J. Galan-Moreno, and E. Rubio-Royo, "Traffic signal optimization in "la almoza" district in saragossa under congestion conditions, using genetic algorithms, traffic microsimulation, and cluster computing," *IEEE Transactions on Intelligent Transportation Systems*, vol. 11, no. 1, pp. 132–141, 2010.
- [17] B. Yin, M. Dridi, and A. EL Moudni, "Traffic control model and algorithm based on decomposition of mdp," in *2014 International Conference on Control, Decision and Information Technologies (CoDIT)*, 2014, pp. 225–230.
- [18] R. Haijema and J. van der Wal, "An mdp decomposition approach for traffic control at isolated signalized intersections," *Probability in the Engineering and Information Sciences*, vol. 22, no. 4, p. 587–602, 2008.
- [19] B. Abdulhai, R. Pringle, and G. Karakoulas, "Reinforcement learning for true adaptive traffic signal control," *Journal of Transportation Engineering*, vol. 129, 05 2003.
- [20] J. Zeng, J. Hu, and Y. Zhang, "Adaptive traffic signal control with deep recurrent q-learning," in *2018 IEEE Intelligent Vehicles Symposium (IV)*, 2018, pp. 1215–1220.

- [21] S. El-Tantawy and B. Abdulhai, "Multi-agent reinforcement learning for integrated network of adaptive traffic signal controllers (marlin-atsc)," 09 2012, pp. 319–326.
- [22] T. Wu, P. Zhou, K. Liu, Y. Yuan, X. Wang, H. Huang, and D. O. Wu, "Multi-agent deep reinforcement learning for urban traffic light control in vehicular networks," *IEEE Transactions on Vehicular Technology*, vol. 69, no. 8, pp. 8243–8256, 2020.
- [23] T. Zhao, P. Wang, and S. Li, "Traffic signal control with deep reinforcement learning," in *2019 International Conference on Intelligent Computing, Automation and Systems (ICICAS)*, 2019, pp. 763–767.
- [24] F. Rasheed, K.-L. A. Yau, R. M. Noor, C. Wu, and Y.-C. Low, "Deep reinforcement learning for traffic signal control: A review," *IEEE Access*, vol. 8, pp. 208 016–208 044, 2020.
- [25] T. Chu, J. Wang, L. Codecà, and Z. Li, "Multi-agent deep reinforcement learning for large-scale traffic signal control," *IEEE Transactions on Intelligent Transportation Systems*, vol. 21, no. 3, pp. 1086–1095, 2020.
- [26] H. Rastgoftar and J.-B. Jeannin, "A physics-based finite-state abstraction for traffic congestion control," *2021 American Control Conference (ACC)*, pp. 237–242, 2021.
- [27] X. Wu, H. X. Liu, and N. Geroliminis, "An empirical analysis on the arterial fundamental diagram," *Transportation Research Part B: Methodological*, vol. 45, no. 1, pp. 255–266, 2011. [Online]. Available: <https://www.sciencedirect.com/science/article/pii/S0191261510000834>
- [28] R. A. Horn and C. R. Johnson, *Matrix Analysis*, 2nd ed. Cambridge University Press, 2012.
- [29] S. Boyd and L. Vandenberghe, *Introduction to Applied Linear Algebra: Vectors, Matrices, and Least Squares*. Cambridge University Press, 2018.
- [30] G. Gu, *Discrete-Time Linear Systems*. Springer US, 2012.

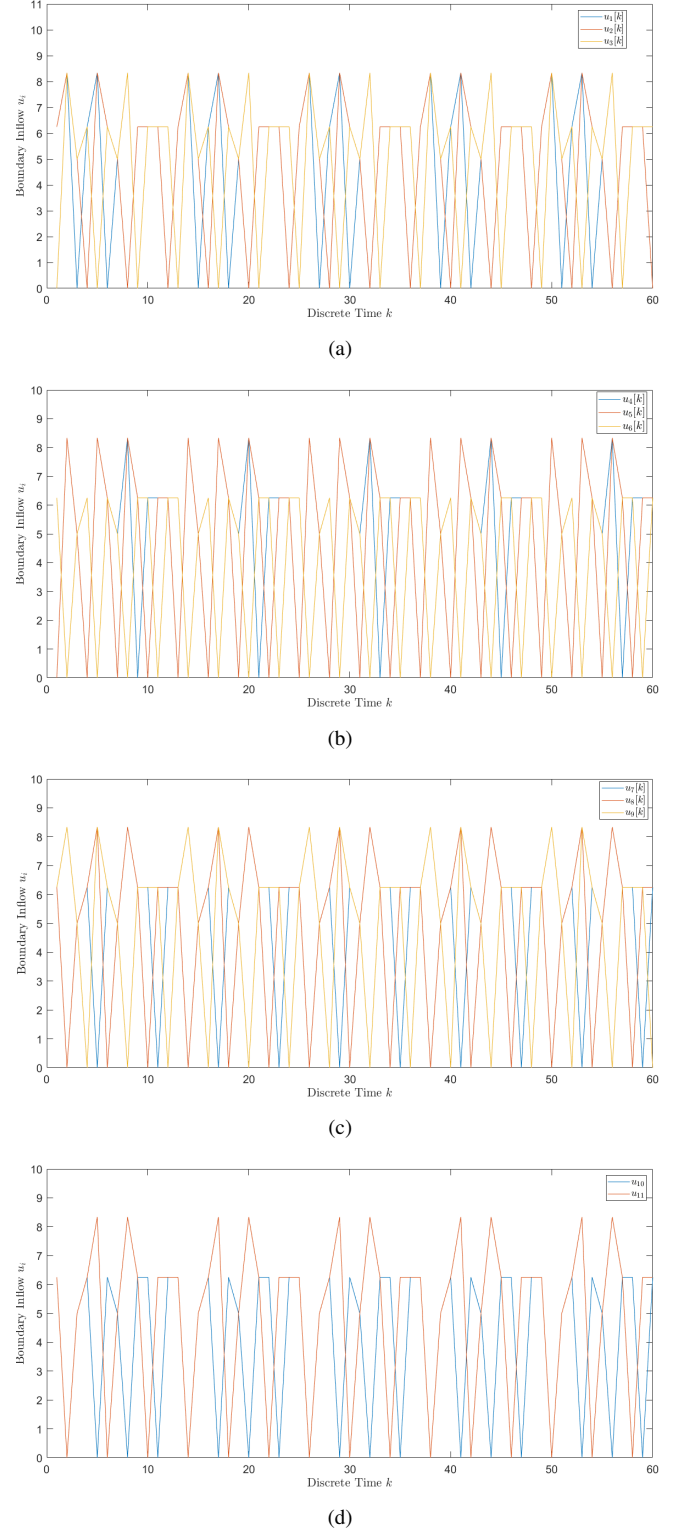


Fig. 6: The optimal boundary inflow at inlet roads (a) $1, 2, 3 \in \mathcal{V}_{in}$, (b) $4, 5, 6 \in \mathcal{V}_{in}$, (c) $7, 8, 9 \in \mathcal{V}_{in}$, and (d) $10, 11 \in \mathcal{V}_{in}$.

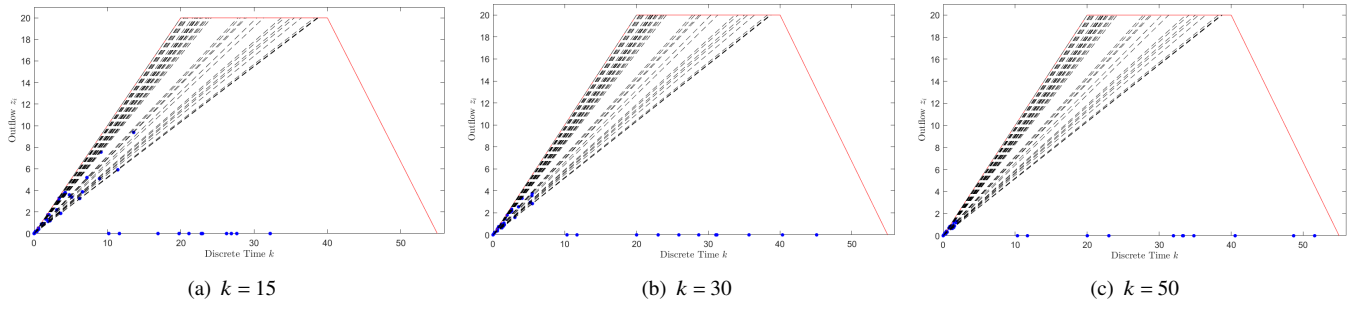


Fig. 7: Outflow of the NOIR roads at (a) $k = 15$, (b) $k = 30$, and (c) $k = 50$.

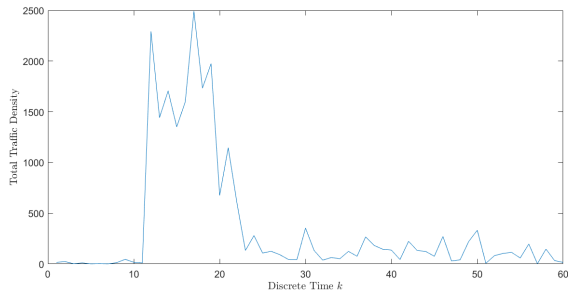


Fig. 8: Schematix of the cyclic graph C_i with movement phase repetition.